ELSEVIER

Chemical Engineering Journal 115 (2005) 93–102

Chemical Engineering Journal

www.elsevier.com/locate/cej

Kinetics of the catalytic hydrogenation of D-fructose over a CuO-ZnO catalyst

Jyrki Kuusisto [a,*], Jyri-Pekka Mikkola [a], Pablo Pérez Casal [a], Hannu Karhu [b], Juhani Väyrynen [b], Tapio Salmi [a]

[a] *Laboratory of Industrial Chemistry, Process Chemistry Centre, Faculty of Chemical Engineering, Åbo Akademi, Biskopsgatan 8, FIN-20500 Turku, Finland*
[b] *Department of Applied Physics, University of Turku, Vesilinnantie 5, FIN-20014 Turku, Finland*

Received 9 May 2005; received in revised form 20 September 2005; accepted 27 September 2005

Abstract

Kinetics of D-fructose hydrogenation over a copper catalyst (61 wt% CuO and 39 wt% ZnO) in aqueous solutions was studied. The hydrogenation experiments were carried out batchwise in a three-phase laboratory-scale reactor (300 ml, Parr Co.), operating at 35–65 bar and between 90 and 130 °C. The main hydrogenation products were mannitol and its epimer, sorbitol. Also, a minor isomerization of fructose to glucose was observed.

In the operating regime studied, the reaction rate showed a second order dependency with respect to the hydrogen pressure. Mannitol selectivity at the experimental range varied from 60 to 68%. The selectivity values improved slightly, as the hydrogen pressure increased or the reaction temperature decreased. The effect of catalyst loading and catalyst deactivation during consecutive hydrogenation batches was also studied. Catalyst characterization studies (nitrogen adsorption BET, XPS, SEM and particle size analysis) were carried out for a better understanding of the catalyst deactivation and reduction processes.

The fitting of the experimental data to the kinetic model was carried out by Modest software using a combined Simplex–Levenberg–Marquardt method. The proposed kinetic model was able to predict the experimental concentrations of fructose and mannitol as well as the by-products sorbitol and glucose with a better than 95% degree of explanation.

Keywords: Catalytic hydrogenation; D-Fructose; D-Mannitol

1. Introduction

The interest towards specialty sugar alcohols has considerably increased during the last years. The exciting functional properties (i.e. anti-caries and other health-related effects) of some products, such as xylitol, have inspired the alimentary and pharmaceutical industry to increase the use of these commodities.

D-Mannitol is widely distributed in the nature (e.g. in olive trees, fruits and vegetables). Mannitol has about half of the sweetness of sucrose and it is least soluble in water of the all commercially used sugar alcohols. Pharmaceutical industry is the largest consumer of mannitol. Due to its low chemical reactivity, low hygroscopicity and excellent mechanical compressing properties, it can be used in the production of chewable tablets and granulated powders as a suitable inert, sweet excipient for both organic and inorganic agents [1]. Moreover, mannitol can be used as an osmotic diuretic [2], in the treatment of cerebral edema [3], for reducing intraocular pressure [4] and as a laxative [5]. The main application for mannitol in the alimentary industry is as a sweetener in sugar-free chewing gums. It is used for powdering and sweetening the surface of diabetic confectionery, because hygroscopic polyols are unsuitable for this purpose [1].

Nowadays, mannitol is usually obtained industrially by catalytic hydrogenation of fructose, sucrose or glucose–fructose syrups [1,6–8]. Hydrolysis of sucrose produces a mixture of glucose and fructose, from which fructose can be separated by chromatography. Higher yields of mannitol are obtained when syrups with high fructose-contents or pure fructose are used. Hydrogenation of fructose over classical nickel-based catalysts gives mannitol yields between 48 and 50 wt%, the other main-product being sorbitol [9,10]. Copper catalysts have a substantially higher selectivity to mannitol [11–14]. Pure mannose is not economically feasible raw material for industry due to

* Corresponding author. Tel.: +358 2 2154574; fax: +358 2 2154479.
E-mail address: jkuusist@abo.fi (J. Kuusisto).

1385-8947/$ – see front matter © 2005 Elsevier B.V. All rights reserved.
doi:10.1016/j.cej.2005.09.020

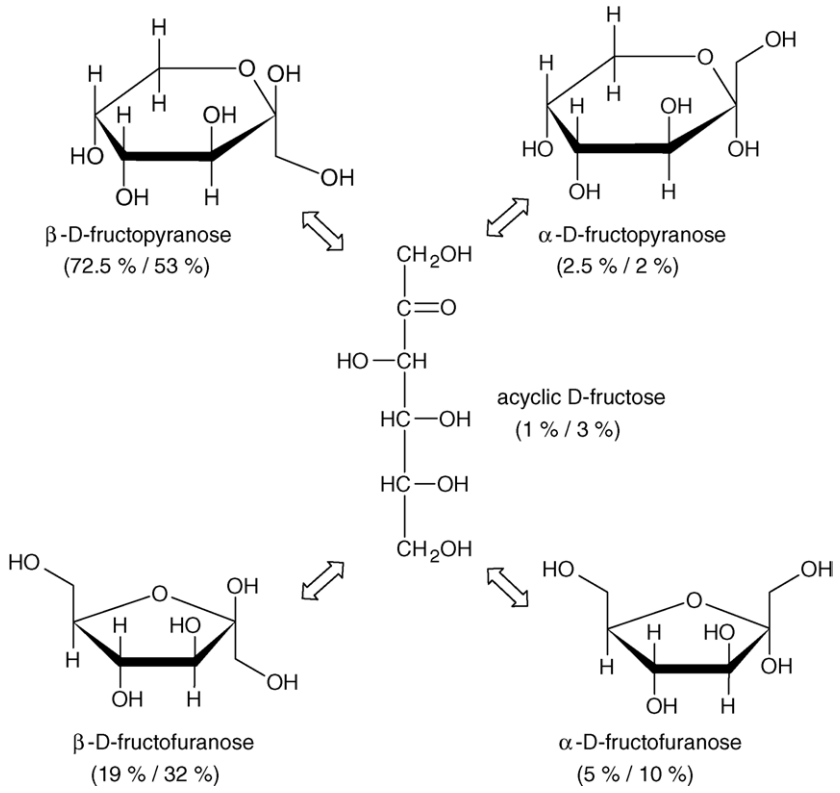

Fig. 1. The fructose mutarotation scheme in water and relative amount of different forms at 20 °C [18] and 80 °C [17].

its high price, despite the fact that mannose leads to a significantly higher mannitol yield. Approximately 30 kt of mannitol was produced worldwide in the year 2000 having 8.0 €/kg as an average market price year 2002. As a comparison, sorbitol was manufactured 900 kt/a, 1.8 €/kg as an average world market price [15].

Pure crystalline fructose exists in the β-pyranose form, while the β-furanose form is most prevalent in naturally occurring oligosaccharides containing fructose units, such as sucrose [16]. In aqueous solutions, acyclic D-fructose is in equilibrium with its four different cyclic forms: β-D-fructopyranose, α-D-fructopyranose, β-D-fructofuranose and α-D-fructofuranose (Fig. 1). The mutarotation equilibrium of fructose solutions is strongly temperature dependent as shown in Fig. 1. The relative amount of furanoses and α-forms of fructose with rising temperature increases. Similar mutarotation equilibrium shift with increased temperature has been observed in NMR studies with xylose [19]. The rate limiting step in the fructose mutarotation is the conversion of β-fructopyranose to the keto form [6]. The furanose–furanose conversion kinetics are much more rapid compared to the pyranose–furanose interconversion and the furanose forms are always in mutual equilibria [20]. However, the interconversion between different D-fructose species is not rate limiting, because the mutarotation rate is much faster compared to the hydrogenation rate [6]. The sugar concentration has been shown to have only a minor impact on the mutarotation equilibrium [21] and interconversion rates [22]. These different tautomeric forms of fructose have different adsorption strengths on the surfaces of hydrogenation catalysts and also individual hydrogenation rates. It is claimed that hydrogenation over Cu and Ni catalysts takes place via the hydrogenation of the ring forms, but not by hydrogenation of the acyclic form. The furanose forms have been found to be more reactive than the pyranose forms [6,12].

The product distribution upon hydrogenation over copper catalysts seems to resemble the β/α-D-fructofuranose ratio. According to one theory, as fructose is hydrogenated, β-fructose molecules are converted to mannitol, while α-fructose molecules give sorbitol as the hydrogenation product [12]. The pyranose form probably plays a minor role in the hydrogenation. Taking into account the somewhat higher adsorption strength of D-glucose (almost 100% in pyranose form) than that of fructose, the small contribution of the pyranose form of D-fructose to the hydrogenation reaction is due to its much lower reactivity [6,14]. Glucose and other by-products may also be produced as fructose is hydrogenated. Proposed D-fructose hydrogenation reaction scheme is displayed in Fig. 2. Reaction temperature, solvent, substrate purity, pH, hydrogen mass transfer and the catalyst composition influence the formation of by-products and the reaction rate.

Hydrogenation kinetics of fructose has been studied over Ru/C [6], Cu/SiO_2 [12] and Raney nickel catalyst [23]. So far, no studies about the use of traditional methanol synthesis catalyst CuO-ZnO for fructose hydrogenation application has been published. Moreover, temperature range in previous fructose hydrogenation studies has been lower. The aim of the present work was to determine the product distribution and hydrogenation kinetics over a commercial CuO-ZnO catalyst.

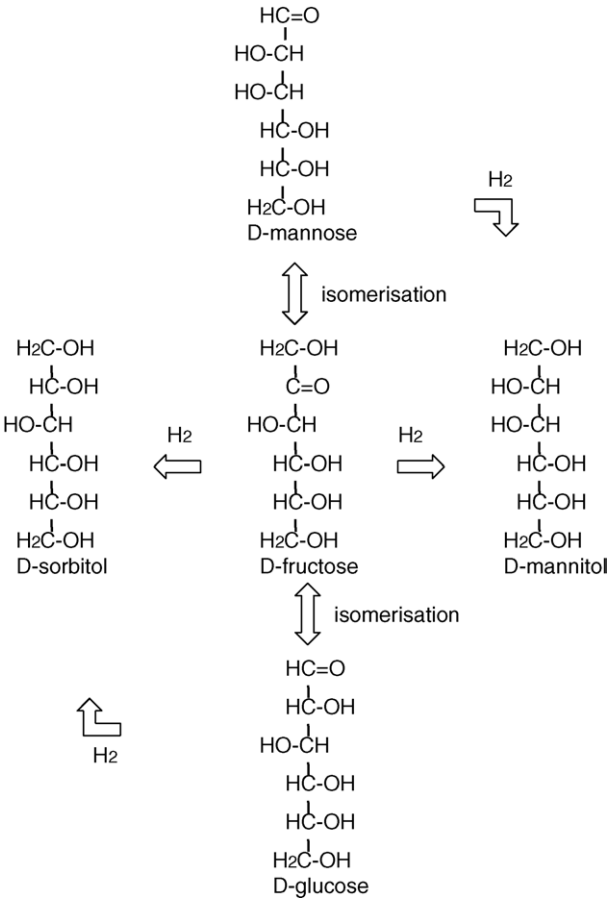

Fig. 2. Fructose hydrogenation scheme.

2. Experimental

The fructose hydrogenation experiments were carried out batchwise in a three-phase laboratory scale reactor (Parr Co.) operating at 35–65 bar and between 90 and 130 °C. The reactor was equipped with a heating jacket, a cooling coil, a filter (0.5 μm metal sinter) in a sampling line and a bubbling chamber (for removing dissolved air from the liquid phase prior hydrogenations). The effective liquid volume of the reactor was about 150 ml (total volume 300 ml) and it was equipped with a hollow shaft concave blade impeller to ensure efficient mixing and gas dispersion into the liquid phase. The stirring rate was 1800 rpm in all of the experiments to operate at the kinetically controlled regime, i.e. in the absence of external mass-transfer limitations. A Parr 4843 controller was used for the temperature control and for monitoring the impeller speed and the pressure in the reactor. The temperature and pressure profiles were recorded in a computer.

A 30 wt% aqueous fructose (Danisco Sweeteners) solution was hydrogenated in all of the experiments, representing industrially relevant concentration regimes. Working with higher concentrations would have caused problems due to the low solubility of mannitol. The solvent used was deionized water and water–ethanol mixture in one experiment. Prior to the first hydrogenation batch, the catalyst from KataLeuna containing 61 wt% CuO and 39 wt% ZnO was reduced in the reactor under hydrogen flow at 300 °C for 2 h (10 bar H_2, heating and cooling rate 5 °C/min). The catalyst amount was varied between 10 and 25 wt% (before reduction) of the fructose weight throughout the kinetic hydrogenation series. The catalyst median particle size was 15.1 μm prior the reduction.

The reactor contents were analysed off-line with a HPLC, equipped with a Biorad Aminex HPX-87C carbohydrate column. A sample for pH measurement was withdrawn simultaneously as the HPLC-sample was taken. An additional sample was withdrawn at the end of the hydrogenation batches to measure the amount of leached metals in the sugar solution. Those samples were filtered with 0.45 μm membrane, diluted with known amount of water and nitric acid was added to ensure that dissolved metals did not precipitate prior to analysis. The dissolved metals were analysed by direct current plasma technique. The state of unreduced, reduced and recycled catalysts was investigated by means of several catalyst characterization techniques: nitrogen adsorption (BET), XPS surface analysis, SEM-EDXA and particle size analysis (Malvern).

3. Kinetic results

The effect of some reaction parameters (stirring rate, reduction temperature and solvent) was studied in the beginning of the work, in order to optimize the hydrogenation of fructose towards mannitol. The conversion and the selectivity values were hardly affected by changing the stirrer speed from 1200 to 1800 rpm as shown in Fig. 3. The stirring speed was, however, fixed at 1800 rpm for the experiments to ensure that the gas–liquid mass transfer does not affect the reaction rate. The water vapour pressure values at different hydrogenation temperatures were estimated according to the Gomez–Thodos method [25,27]. The values of estimated vapour pressures were used for calculation of partial hydrogen pressures at different reaction temperatures given in Table 1.

Internal mass transfer inside the catalyst particles was determined by calculation of the catalyst effectiveness factor η_{eff} [25,26]. Calculation of η_{eff} under reaction conditions gave η_{eff} close value 1, indicating that hydrogen diffusion inside the catalyst pores does not affect the reaction rate. In general, diffusion

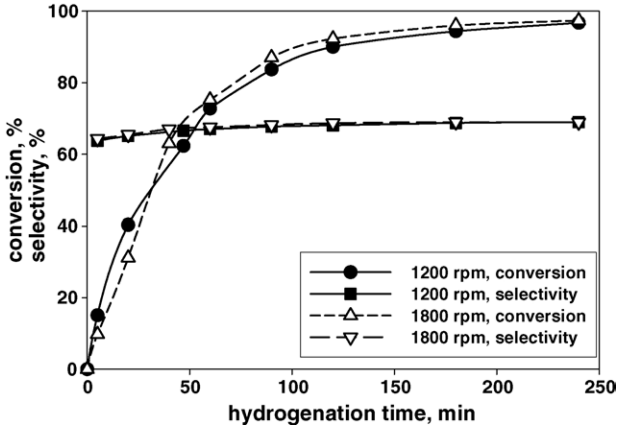

Fig. 3. The effect of the impeller speed on the hydrogenation of fructose to mannitol.

Table 1
Partial hydrogen pressures (bar) at different hydrogenation experiments

Total pressure (bar)	90 °C	110 °C	130 °C
35	–	33.65	32.72
50	49.25	48.65	47.72
65	–	63.65	62.72

Table 2
Evaluation of the role of intraparticular diffusion

T (°C)	130
R' (mol/(h g_{CAT}))	0.0324
C_{TOT} (mol/l)	43.21
D_{H_2} (m^2/s)	1.09×10^{-8}
ε_P	0.5
ρ_P (kg/m^3)	850
η_{eff}	0.9994
p (bar)	65
R_P (μm)	7.55
x_{H_2}	5.81×10^{-4}
D_{eff,H_2} (m^2/s)	1.82×10^{-9}
τ_P	3
ϕ	0.098

effect increases as the reaction rate increases. Thus, the observed initial rate and other physical parameters at the highest pressure (65 bar) and temperature (130 °C) were used in calculations. The results from the evaluation of the role of intraparticular diffusion are summarized in Table 2. The diffusion coefficient of hydrogen in the reaction solution was estimated according to Wilke–Chang equation

$$D_{Am} = \frac{7.4 \times 10^{-12} (\sum_{i=1}^{n} x_i \phi_i M_i)^{1/2} T}{\eta_m V_A^{0.6}} \text{ m}^2/\text{s} \quad (1)$$

where x_i is the mole fraction of each compound, ϕ_i the association factor (2.6 for water and 1.0 for unassociated solvents), M_i the molecular weight (18.02 g/mol for water and 180.16 g/mol for fructose), η_m the dynamic viscosity of fructose solution and $V_A = 14.3\ \text{cm}^3/\text{g}$ for hydrogen [28]. The dynamic viscosity of 30 wt% fructose solution was estimated from equations derived for sucrose solutions [29] and was estimated to vary between 0.73 and 0.40 cP from 90 to 130 °C. The calculations indicate that the diffusion coefficient of hydrogen varies between 5.4×10^{-9} and $1.09 \times 10^{-8}\ \text{m}^2/\text{s}$ at the temperature range from 90 to 130 °C. The hydrogen concentration in fructose hydrogenation solutions was calculated from a correlation based on experimental determination of hydrogen solubility in aqueous sugar–sugar alcohol solutions

$$C_H = \frac{x_F}{x_F + x_M}\left[\ln(0.9991) - \frac{0.1144}{T/K} + 0.0004228\ \ln(p_H\,(\text{bar}))\right] + \frac{x_M}{x_F + x_M}\left[\ln(0.9993) - \frac{0.11603}{T/K} + 0.00041126\ \ln(p_H\,(\text{bar}))\right] \quad (2)$$

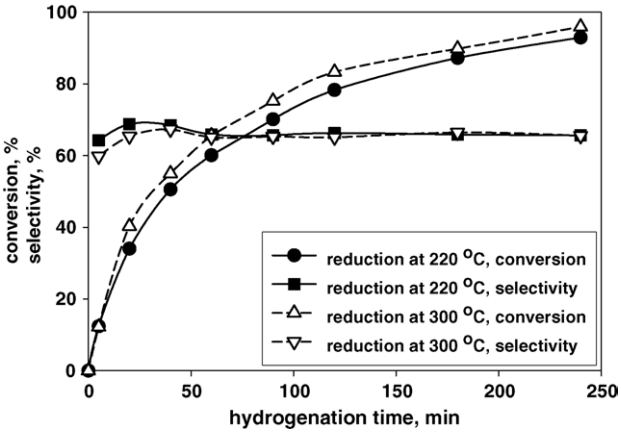

Fig. 4. The effect of the reduction temperature on the hydrogenation of fructose to mannitol.

where x_F and x_M represent the relative amounts of fructose and mannitol in hydrogenation mixture [26].

Concerning the effect of the catalyst reduction temperature, somewhat improved results were achieved as the temperature was increased from 220 to 300 °C as revealed by Fig. 4. Higher reduction temperatures would have lead to a more severe loss of active metal surface area via sintering. The influence of the catalyst loading on the fructose hydrogenation kinetics was studied as well. The initial reaction rate showed a linear dependency on the catalyst load between 10 and 25 wt% of fructose amount, i.e. the hydrogenation was first order with respect to catalyst amount at the experimental range (Fig. 5). Nevertheless, a further increase of the catalyst load did not give a full benefit. Thus, the system was not anymore in the kinetic regime and the liquid–solid mass transfer started to influence the reaction rate.

A water–ethanol mixture (70/30 wt% ratio) was compared to pure water in fructose hydrogenation. The higher solubility of hydrogen in alcohols could in principle give an improved reaction rate. Nevertheless, the water–ethanol mixture had a negative impact on the average hydrogenation rate and the mannitol selectivity (Fig. 6). However, initial reaction rates were comparable and it seems that the low mannitol solubility started disturbing

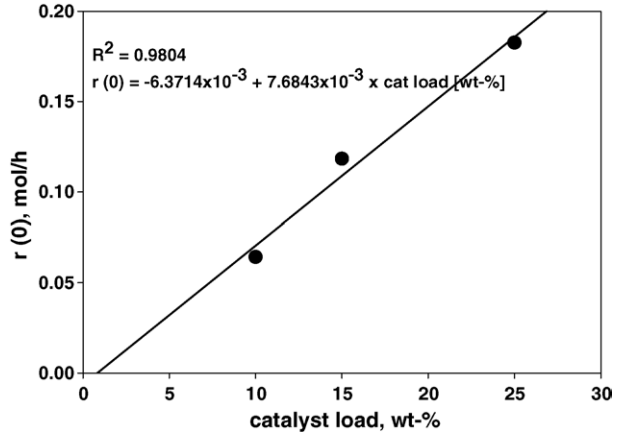

Fig. 5. The influence of catalyst loading on the initial reaction rate at 110 °C and 50 bar.

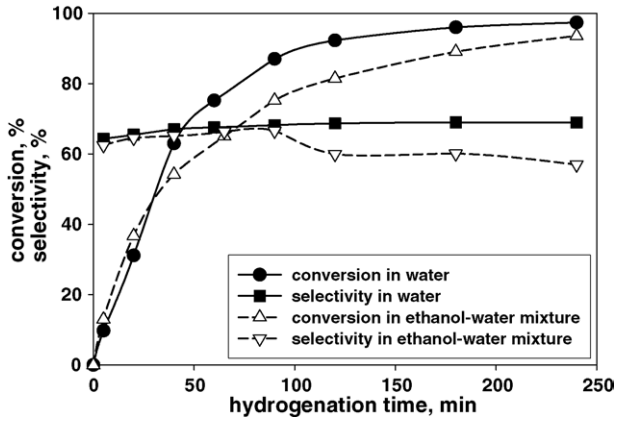

Fig. 6. Solvent influence on the hydrogenation of fructose to mannitol.

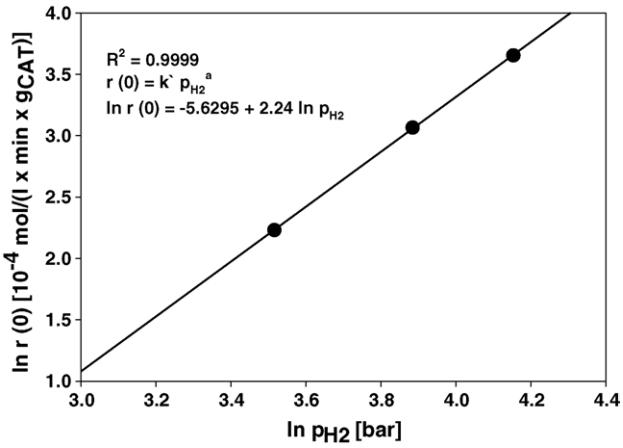

Fig. 8. Determination of the reaction order with respect to hydrogen pressure at 110 °C.

the reaction and the HPLC-analysis at the end of batch. Moreover, it has been proved that the rate of fructose mutarotation decreases as the concentration of ethanol in the solvent increases [20]. Also, fructose solubility in alcohol solutions is known to be relatively poor and the viscosity of the aqueous-alcoholic sugar solution is higher than that of aqueous. These phenomena might explain the diminished reaction rate in the alcoholic solvent.

The effect of the reaction temperature on the fructose hydrogenation rate was clear. The hydrogenation rate was clearly improved at higher reaction temperatures as shown in Fig. 7. An increased hydrogen pressure had a positive effect on the initial reaction rate, showing a second order behaviour at 110 °C (Fig. 8). Only hydrogenation experiment at 35 bar and 130 °C differed clearly from the other runs, because diffusion limitations of hydrogen started probably influence the reaction in the beginning of batch. Also, clearly more glucose was formed at the hydrogenation at 35 bar and 130 °C. Under hydrogen poor conditions, glucose molecules are easily dehydrogenated, leading to gluconic acid formation. This reaction mechanism can be explained as the so called oxidative dehydrogenation or transfer hydrogenation [30,34], where simultaneously one glucose molecule is dehydrogenated and other one reduced to sorbitol. Obviously, it is not correct to denote the reaction as a Cannizzaro reaction, since only aldehydes without hydrogen in α-position are subject to the Cannizzaro reaction in strongly alkaline solution [35]. In aqueous, alkaline medium under ambient conditions, D-fructose is hydrogenated rapidly, D-mannose rather slowly and D-glucose is dehydrogenated mainly to gluconic acid and reduced to D-sorbitol [34]. Formation of D-gluconic acid is known to deactivate catalysts by blocking the active sites [30,31]. D-Gluconic acid is also a strong chelating agent, which increases leaching of metals. These facts support the theory that gluconic acid was formed upon hydrogenations at low hydrogen pressures and high temperatures, because at such conditions pH drop was more severe (Fig. 10) and catalyst leaching increased. Also, more glucose was formed at hydrogen poor conditions. The mannitol selectivity improved slightly, as the hydrogen pressure was increased and the reaction temperature decreased. The sorbitol-to-mannitol ratio remained constant during the entire hydrogenation time of each experiment (Fig. 9). The mannitol selectivity at the experimental range varied from 60 to 68%.

In dilute basic solutions fructose epimerizes to glucose and mannose according to Lobry de Bruyn–van Ekenstein

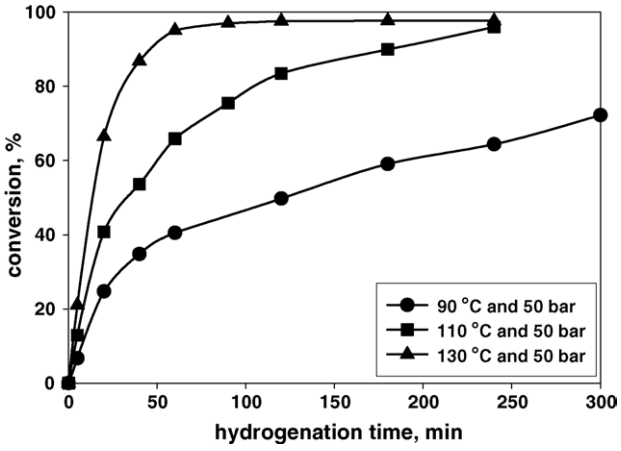

Fig. 7. The influence of reaction temperature on the fructose hydrogenation rate.

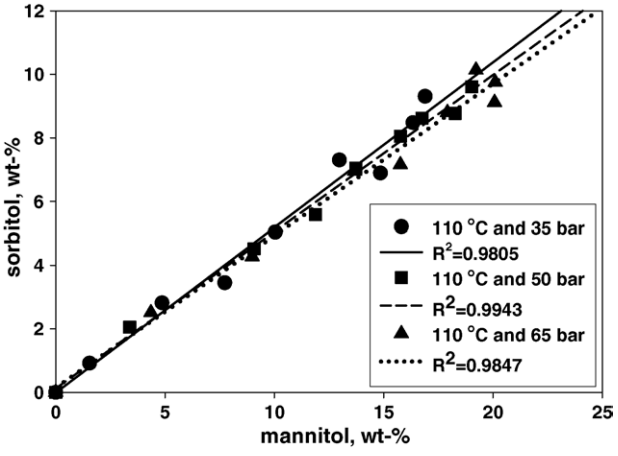

Fig. 9. The effect of hydrogen pressure on the sorbitol/mannitol ratio during the reactions.

reaction [24]. In these kinetic experiments, glucose was formed 0.3–1.9 wt%, in the beginning of the hydrogenations and this concentration remained almost unchanged towards the end of the reaction, at hydrogenations between 90 and 110 °C. In fructose hydrogenations at 130 °C, the amount of glucose decreased towards the end of the reaction. Mannose formation was below the detection limit in all of these experiments, since it was presumably hydrogenated rapidly to mannitol.

4. Catalyst stability

According to the direct current plasma measurements, copper leaching was always minor, but severe zinc leaching was observed during hydrogenations. Lower hydrogenation pressure and higher reaction temperature increased the amount of dissolved zinc. It was also observed that in such conditions, the pH value of the hydrogenation solution decreased more significantly during the reaction (Fig. 10). The catalyst leaching values at the end of kinetic hydrogenation batches are summarized in Table 3.

The CuO/ZnO catalyst was reused in four consecutive batches to obtain information about its deactivation. Quite substantial decrease in the catalyst activity was observed as well as slightly decreased mannitol selectivity from batch to batch

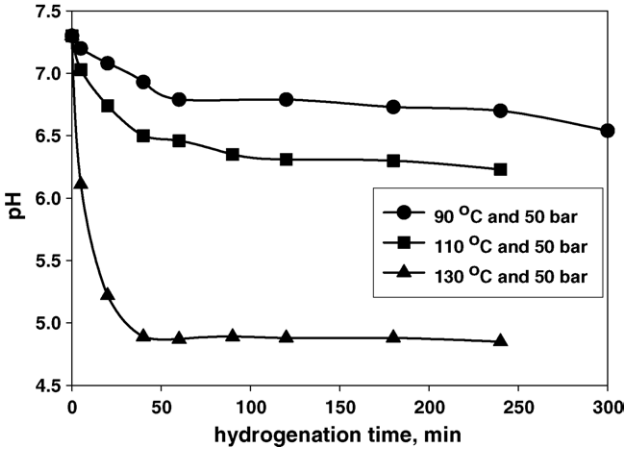

Fig. 10. Evolution of pH in fructose hydrogenations performed at different temperatures.

Table 3
Leached metals at the end of different hydrogenation batches

T (°C)	p_{TOT} (bar)	Cu (mg/l)	Zn (mg/l)	Batch no.
90	50	1.6	56.7	1
110	35	1.7	314.1	1
110	50	1.8	227.0	1
110	65	2.8	155.4	1
130	35	2.3	1316.8	1
130	50	1.8	467.8	1
130	65	1.7	350.1	1
110	50	2.4	228.4	1
110	50	2.2	267.6	2
110	50	2.5	311.3	3
110	50	1.6	337.3	4

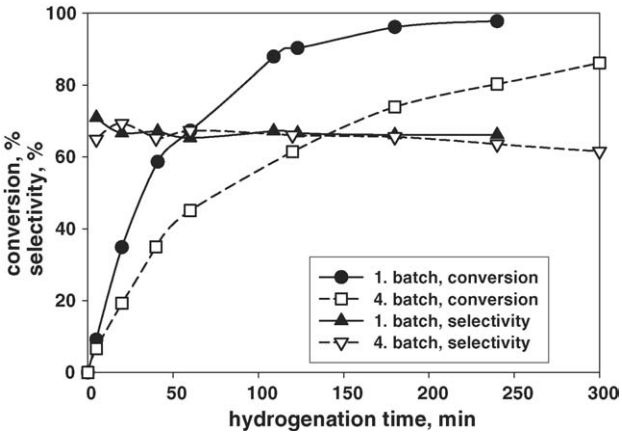

Fig. 11. Conversion and selectivity values obtained in the deactivation study performed at 110 °C and 50 bar.

(Fig. 11). The zinc leaching increased in each consecutive batch as the catalyst was recycled (Table 3).

5. Catalyst characterization results

Catalyst reduction at 300 °C reduced the specific surface area and pore volume remarkably probably due to sintering. Recycling of the catalyst in four consecutive hydrogenation batches reduced further the surface area due to the pore blockage. Table 4 displays the results of the nitrogen adsorption experiments.

Surface analysis (XPS) of both fresh and reduced catalyst samples were performed. In a fresh catalyst sample, Cu^{2+} (CuO and $Cu(OH)_2$) was the predominant Cu species. Zinc was present in two separate oxidation states, mainly as ZnO. During the catalyst reduction procedure, Cu^{2+} was fully reduced to metallic Cu^0. Zinc was not reduced during the catalyst activation to a significant degree. The relative atomic ratio on the catalyst surface was Cu/Zn = 0.70 after reduction. Fig. 12 shows a comparison of the oxidation states between fresh and reduced catalysts.

The particle size distributions of fresh, reduced and recycled catalysts were measured by Malvern 2600 (Table 4). The particle size measurements support the conclusion that metal sintering takes place during the catalyst reduction since the median particle size increased during catalyst activation. The amount of catalyst fines increased as the catalyst was recycled in four consecutive batches, most probably due to attrition. Same changes in catalyst particle sizes were visible in SEM pictures too.

Table 4
Results of the nitrogen adsorption and particle size distribution analysis

Catalyst sample	Fresh	Reduced	Recycled
Specific surface area (m^2/g)	50.71	21.39	12.96
Pore volume (ml/g)	0.2251	0.1125	0.0900
D_{50} (μm)	15.1	17.6	15.6
D_{10} (μm)	4.9	3.5	3.0
D_{90} (μm)	34.1	54.1	49.1

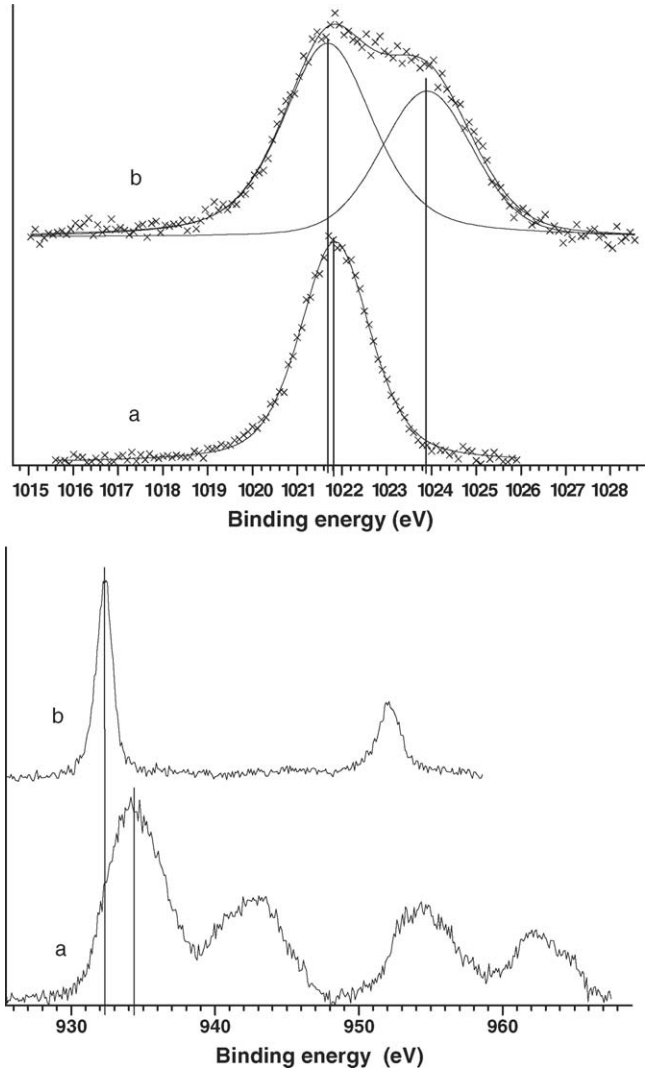

Fig. 12. In the picture highest up is the Cu 2p X-ray photoelectron line for (a) fresh and (b) reduced catalyst. In the picture below is displayed the Zn $2p_{3/2}$ line for the same catalysts.

6. Kinetic modelling

The Langmuir–Hinshelwood–Hougen–Watson (LHHW) approach is based on the Langmuir model describing the surface of a catalyst as an array of equivalent sites that do not interact either before or after chemisorption. Moreover, it is assumed that both reactants and products are in equilibria with surface species that react on the surface in rate-determining steps. The surface coverages are correlated to the partial pressures or concentrations in the fluid phase by means of Langmuir adsorption isotherms. The Langmuir model is unrealistic from a theoretical viewpoint, since the surface coverages are by no means identical to the equilibrium values predicted by the Langmuir adsorption isotherm for reaction systems in which kinetic coupling occurs. Despite this weakness, the LHHW kinetics has proved valuable for modelling heterogeneous catalytic reactions for reactor and process design.

The surface reactions between adsorbed species, i.e. fructose and hydrogen, were presumed to be the rate-determining steps, and the remaining ones were assumed to proceed rapidly. In accordance with some studies [23], the organic molecules and the hydrogen atoms compete for different kind of active sites. However, a competitive adsorption model, in which all the species occupy the same type of sites, was applied here. The reaction steps and rate equations were derived according a principle shown in reference [19]. The adsorption of hydrogen was assumed to be dissociative. Nevertheless, the hydrogen atoms were presumed to be added pairwise to the carbonyl group. Since, the rate, adsorption and isomerization constants are dependent on the temperature, a kinetic model was constructed in order to estimate the pre-exponential factors of these constants. The model predicts the same reaction orders for both mannitol and sorbitol formation, according to the real product distribution (Fig. 9).

The fitting of the experimental data to the kinetic model was carried out by Modest (MOdel ESTimation) software using a combined Simplex–Levenberg–Marquardt method [32]. The differential equations describing the mass balances of the organic components were solved by the backward-difference method during the parameter estimation [33]. Because of the absence of severe external mass transfer limitations, the concentration of dissolved hydrogen was obtained directly from Eq. (2). The estimation of the parameters was based on simultaneous fitting of the multiple data sets, i.e. the experiments performed at various temperatures and pressures. Based on previous knowledge, some of the parameters were fixed at certain initial values, meanwhile the others were allowed to change. The following objective function was used in data fitting:

$$Q = \sum (C_{i,\mathrm{exp}} - C_{i,\mathrm{calc}})^2 w_i \tag{3}$$

where the weight factors were chosen as follows: $w = 1$ for fructose, mannitol and sorbitol, and $w = 5$ for glucose. Weighting was beneficial to enhance the influence of glucose concentration in the estimation, since it was present in considerably lower concentrations than the main products and the reactant. The quality of the data fitting was controlled by using the degree of explanation (R^2), defined as follows:

$$R^2 = 1 - \frac{\sum (C_{i,\mathrm{exp}} - C_{i,\mathrm{model}})^2}{\sum (C_{i,\mathrm{exp}} - C_{i,\mathrm{mean}})^2} \tag{4}$$

where $C_{i,\mathrm{mean}}$ indicates the average value of the experimental values.

Fig. 13 illustrates the fit of the kinetic model to the experimental data in the different experiments carried out. The figures reveal that the kinetic model is able to predict the experimental concentrations quite well. The overall degree of explanation of the obtained fit, taking into account all the experiments performed, was 95.6%. As the experiment carried out at 130 °C and 35 bar H_2 pressure was not included in the model, the degree of explanation increased to 98.0%. Evidently the data were not stoichiometrically consistent at 130 °C and 35 bar, as indicated by the Fig. 13. The difference between the activation energies of the hydrogenation of fructose to mannitol and sorbitol can be estimated from the values obtained in the kinetic model ($E_{a2} - E_{a1} = 4.1$ kJ/mol). The value obtained from this

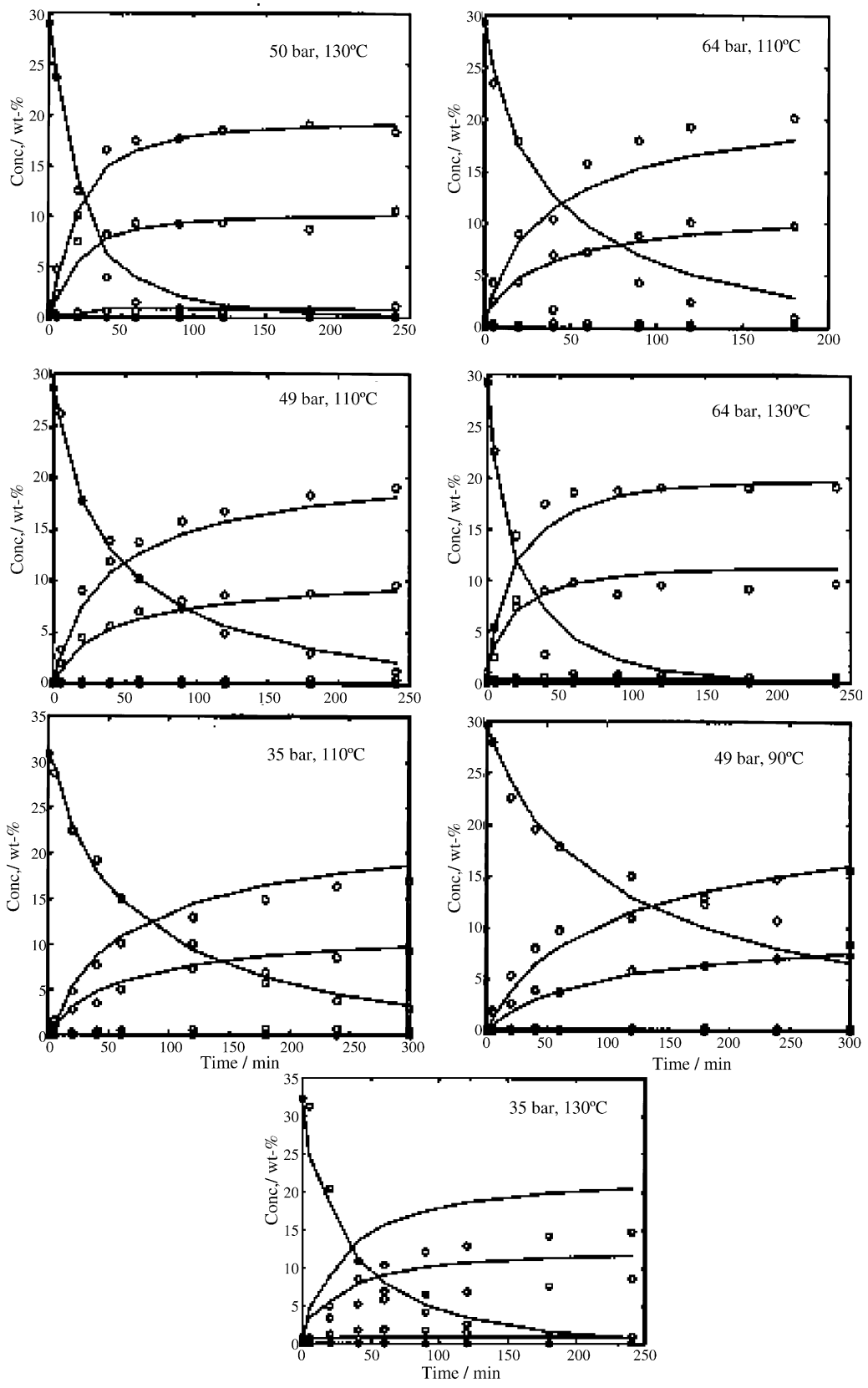

Fig. 13. Kinetic curves of fructose hydrogenation experiments at different temperature and pressure values (◯, experimental values; —, model fit).

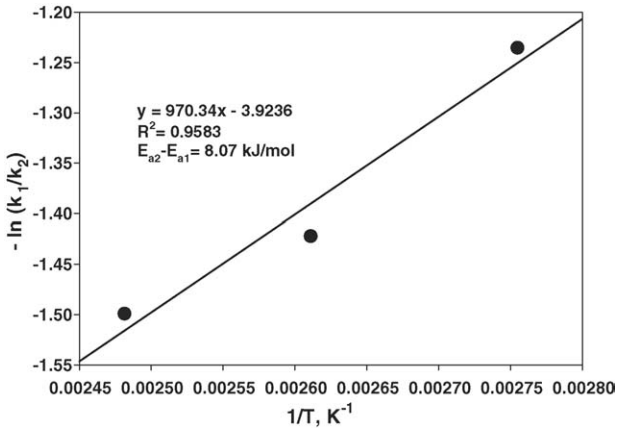

Fig. 14. Estimation of ($E_{a2} - E_{a1}$) from the experiments performed at different reaction temperatures.

estimation is in the same order of magnitude as the one obtained from Fig. 14 ($E_{a2} - E_{a1}$ = 8.07 kJ/mol) calculated on the basis of the experiments carried out at different temperatures. As it was mentioned before, the temperature does not have an essential influence in the selectivity of the fructose hydrogenation towards mannitol or sorbitol, but an increase in the reaction temperature will slightly benefit the production of sorbitol, due to the higher value of E_{a2}.

7. Conclusions

According to the measurements carried out at the laboratory, the catalyst reduction at 300 °C diminished the surface area by 57.8% and the pore volume 50% due to sintering. The surface area was further reduced by 39.4% after hydrogenating four consecutive batches fructose, mainly due to pore blockage. The drop of initial reaction rate from first to fourth batch was 29.4% and thus of similar order of magnitude than decrease of active catalyst surface area. The reasons for pore blockage were presumably the leaching and back-precipitation of the zinc on the catalyst surface. Moreover, metal complexes between zinc and some hydrogenation products, such as gluconic acid, were presumably formed. The decreased catalyst surface area combined with partial catalyst oxidation and poisoning of active sites were explanations for the catalyst deactivation.

The initial fructose hydrogenation rates proved to be second order with respect to hydrogen pressure. An increase of both temperature and pressure had a positive effect on reaction rate within the experimental range. The mannitol selectivity values improved slightly, as hydrogen pressure was increased and the reaction temperature decreased. The fact that relative amount of α-fructose increases at higher temperatures, could explain decreased mannitol selectivity with increasing hydrogenation temperature. Furthermore, furanoses are known to be more reactive than pyranoses, which might partially explain the enhancement of the hydrogenation rate with increasing temperature. Decreased hydrogen pressure and increased reaction temperature led to higher zinc leaching. Copper leaching was always minor, but zinc dissolved remarkably and leaching increased in every hydrogenation batch, as the same catalyst was used in four consecutive batches. Amount of the catalyst fines increased as the catalyst was recycled, probably due to attrition.

A kinetic model was developed and it was able to predict the experimental concentrations, the fructose conversion and the product distribution rather well. The overall degree of explanation of the obtained fit, taking into account all the experiments performed, was 95.6%.

Acknowledgements

This work is part of the activities at the Åbo Akademi Process Chemistry Centre within the Finnish Centre of Excellence Programme (2000–2005) by the Academy of Finland. Financial support of the National Technology Agency (Tekes), Danisco Sweeteners and Swedish Academy of Engineering Sciences in Finland is gratefully acknowledged.

References

[1] E. Schwartz, Sugar Alcohols: Mannitol, Ullmann's Encyclopedia of Industrial Chemistry, vol. 34, sixth ed., VCH, Weinheim, 2003.
[2] L. Gever, Mannitol: the osmotic diuretic of choice, Nursing 15 (7) (1985) 64.
[3] F. Heppner, G. Lanner, L. Auer, The treatment of traumatic brain edema, Wien. Med. Wochenschr. 126 (1976) 105–109.
[4] U. Hase, H.I. Reulen, Influence of sorbitol and mannitol on intracranial pressure, Neurochirurgia 23 (6) (1980) 205–211.
[5] K.R. Palmer, A.N. Khan, Oral mannitol: a simple and effective bowel preparation for barium edema, Br. Med. J. 2 (1979) 1038.
[6] A.W. Heinen, J.A. Peters, H. van Bekkum, Hydrogenation of fructose on Ru/C catalysts, Carbohydr. Res. 328 (2000) 449–457.
[7] A.W. Heinen, J.A. Peters, H. van Bekkum, The combined hydrolysis and hydrogenation of inulin catalyzed by bifunctional Ru/C, Carbohydr. Res. 330 (2001) 381–390.
[8] H. Ojamo, H. Koivikko, H. Heikkilä, Process for the production of mannitol by immobilized micro-organisms, Patent WO 0004181 (2000).
[9] F. Devos, Process for manufacture of mannitol, US patent US 5466795 (1995).
[10] M. Makkee, A.P.G. Kieboom, H. van Bekkum, Production methods of D-mannitol, Starch 37 (1985) 136–141.
[11] M. Hegedüs, S. Göbölös, J.L. Margitfalvi, Stereoselective hydrogenation of D-fructose to D-mannitol on skeletal and supported copper-containing catalysts, Stud. Surf. Sci. Catal. 78 (1993) 187–194.
[12] M. Makkee, A.P.G. Kieboom, H. van Bekkum, Hydrogenation of D-fructose and D-fructose/D-glucose mixtures, Carbohydr. Res. 138 (1985) 225–236.
[13] J.F. Ruddlesden, A. Stewart, D.J. Thompson, R. Whelan, Diastereoselective control in ketose hydrogenations with supported copper and nickel catalysts, Faraday Discuss. Chem. Soc. 72 (1981) 397–411.
[14] M. Makkee, Combined action of Enzyme and Metal Catalyst, applied to the preparation of D-Mannitol, Doctoral Thesis, Technische Hogeschool Delft, 1984.
[15] F.W. Lichtenthaler, Carbohydrates, Ullmann's Encyclopedia of Industrial Chemistry, vol. 6, sixth ed., VCH, Weinheim, 2003.
[16] K. Heyns, D-Fructose—structure and properties, Starch 30 (1978) 345–351.
[17] S.J. Angyal, The composition of reducing sugars in solution, Adv. Carbohydr. Chem. Biochem. 42 (1984) 15–68.
[18] B. Schneider, F.W. Lichtenthaler, G. Steinle, H. Schiweck, Studies on ketoses, Liebigs Ann. Chem. 12 (1985) 2443–2453.
[19] J.-P. Mikkola, R. Sjöholm, T. Salmi, P. Mäki-Arvela, Xylose hydrogenation: kinetic and NMR studies of the reaction mechanisms, Catal. Today 48 (1999) 73–81.

[20] A.E. Flood, M.R. Johns, E.T. White, Mutarotation of D-fructose in aqueous-ethanolic solutions and its influence on crystallisation, Carbohydr. Res. 288 (1996) 45–56.
[21] L. Hyvönen, P. Varo, P. Koivistoinen, Tautomeric equilibria of D-glucose and D-fructose: NMR spectrometric measurements, J. Food Sci. 42 (1977) 657–659.
[22] G. Haase, T.A. Nickerson, Kinetic reactions of alpha and beta lactose. I. Mutarotation, J. Dairy Sci. 49 (1966) 127–132.
[23] H.C.M. Pijnenburg, B.F.M. Kuster, H.S. van der Baan, Kinetics of the hydrogenation of fructose with Raney-nickel, Starch 30 (10) (1978) 352–355.
[24] P. Collins, R. Ferrier, Monosaccharides, Their Chemistry and Their Roles in Natural Products, John Wiley & Sons Ltd., England, 1995, p. 139.
[25] J. Hájek, D. Yu. Murzin, Liquid phase hydrogenation of cinnamaldehyde over Ru-Sn sol–gel catalyst. 1. Evaluation of mass transfer via combined experimental/theoretical approach, Ind. Eng. Chem. Res. 43 (2004) 2030–2038.
[26] J.-P. Mikkola, T. Salmi, R. Sjöholm, Kinetic and mass-transfer effects in the hydrogenation of xylose to xylitol, Stud. Surf. Sci. Catal. 122 (1999) 351–358.
[27] R.C. Reid, J.M. Prausnitz, B.E. Poling, The Properties of Gases and Liquids, McGraw-Hill, New York, 1988.
[28] C.R. Wilke, P. Chang, Correlation of diffusion coefficients in dilute solutions, AIChE J. 1 (1955) 264–270.
[29] J. Laine, Nesteiden ainearvot prosessilaskentaa varten, Tampere (1999).
[30] B.W. Hoffer, E. Crezee, F. Devred, P.R.M. Mooijman, W.G. Sloof, P.J. Kooyman, A.D. van Langeveld, F. Kapteijn, J.A. Moulijn, The role of the active phase of Raney-type Ni catalysts in the selective hydrogenation of D-glucose to D-sorbitol, Appl. Catal. A 253 (2003) 437–452.
[31] B. Arena, Deactivation of ruthenium catalysts in continuous glucose hydrogenation, Appl. Catal. A 87 (1992) 219–229.
[32] H. Haario, MODEST User's Manual, Profmath Oy, Helsinki, 1994.
[33] C.W. Gear, Numerical Initial Value Problems in Ordinary Differential Equations, Prentice Hall, New Jersey, 1971.
[34] G. de Wit, J.J. de Vlieger, A.C. Kock-van Dalen, R. Heus, R. Laroy, A.J. van Hengstum, A.P.G. Kieboom, H. van Bekkum, Catalytic dehydrogenation of reducing sugars in alkaline solution, Carbohydr. Res. 91 (1981) 125–138.
[35] Y. Önal, S. Schimpf, P. Claus, Structure sensitivity and kinetics of D-glucose oxidation to D-gluconic acid over carbon-supported gold catalysts, J. Catal. 223 (2004) 122–133.